Lagrangian Decomposition of the Meridional Heat Transport at 26.5°N

Oliver John Tooth[1], Nicholas P. Foukal[2], William E. Johns[3], Helen Louise Johnson[1], and Chris Wilson[4]

[1]University of Oxford
[2]Woods Hole Oceanographic Institution
[3]Rosenstiel School of Marine and Atmospheric Science, University of Miami
[4]National Oceanography Centre

November 22, 2023

Abstract

The Atlantic Meridional Overturning Circulation (AMOC) plays a critical role in the global climate system through the redistribution of heat, freshwater and carbon. At 26.5°N, the meridional heat transport has traditionally been partitioned geometrically into vertical and horizontal circulation contributions; however, attributing these components to the AMOC and Subtropical Gyre (STG) flow structures remains widely debated. Using water parcel trajectories evaluated within an eddy-rich ocean hindcast, we present the first Lagrangian decomposition of the meridional heat transport at 26.5°N. We find that water parcels recirculating within the STG account for 37% (0.36 PW) of the total heat transport across 26.5°N, more than twice that of the classical horizontal "gyre" component (15%). Rather than being distinct from the overturning circulation, the heat transport associated with the STG is due to the formation of subtropical mode waters via a shallow downward spiral, which ultimately feeds the northward limb of the AMOC.

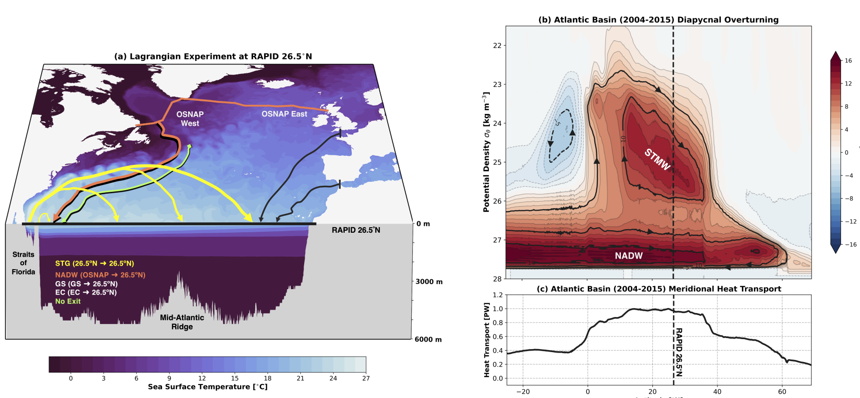

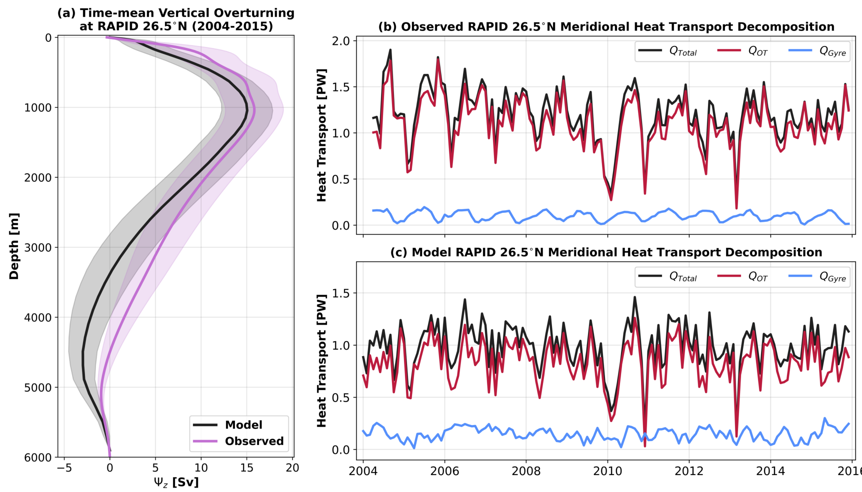
(a) Time-mean Vertical Overturning at RAPID 26.5°N (2004-2015)
Depth [m]
Ψz [Sv]
Model
Observed
(b) Observed RAPID 26.5°N Meridional Heat Transport Decomposition
Heat Transport [PW]
Q_Total
Q_OT
Q_Gyre
(c) Model RAPID 26.5°N Meridional Heat Transport Decomposition
Heat Transport [PW]
Q_Total
Q_OT
Q_Gyre

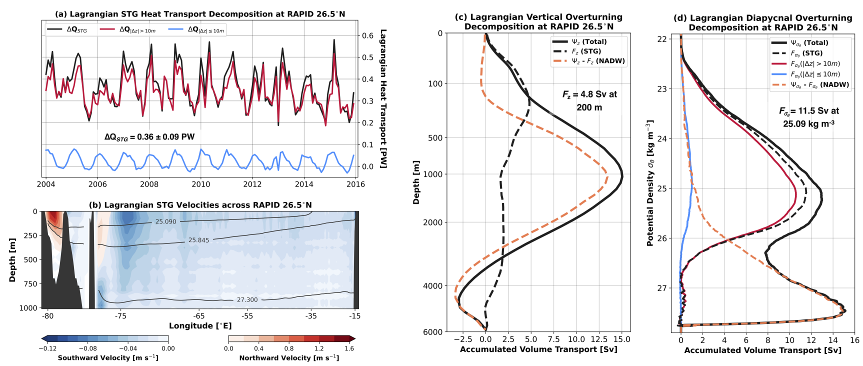
(a) Lagrangian STG Heat Transport Decomposition at RAPID 26.5°N
Lagrangian Heat Transport [PW]
ΔQ_STG = 0.36 ± 0.09 PW
(b) Lagrangian STG Velocities across RAPID 26.5°N
Depth [m]
Longitude [°E]
Southward Velocity [m s⁻¹]
Northward Velocity [m s⁻¹]
(c) Lagrangian Vertical Overturning Decomposition at RAPID 26.5°N
Ψz (Total)
Fz (STG)
Ψz - Fz (NADW)
Fz = 4.8 Sv at 200 m
Depth [m]
Accumulated Volume Transport [Sv]
(d) Lagrangian Diapycnal Overturning Decomposition at RAPID 26.5°N
Potential Density σ0 [kg m⁻³]
Fσ0 = 11.5 Sv at 25.09 kg m⁻³
Accumulated Volume Transport [Sv]

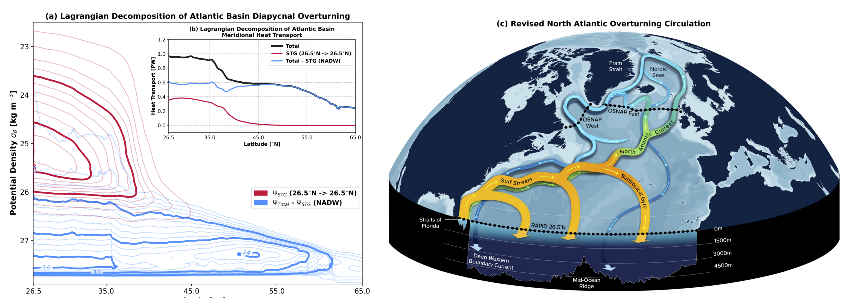
(a) Lagrangian Decomposition of Atlantic Basin Diapycnal Overturning
(b) Lagrangian Decomposition of Atlantic Basin Meridional Heat Transport
Heat Transport [PW]
Latitude [°N]
Potential Density σ0 [kg m⁻³]
Latitude [°N]
(c) Revised North Atlantic Overturning Circulation
Fram Strait
Nordic Seas
OSNAP West
OSNAP East
North Atlantic Current
Gulf Stream
Subtropical Gyre
Straits of Florida
RAPID 26.5°N
Deep Western Boundary Current
Mid-Ocean Ridge
0m
1500m
3000m
4500m

Lagrangian Decomposition of the Meridional Heat Transport at 26.5°N

Oliver J. Tooth[1], Nicholas P. Foukal[2], William E. Johns[3], Helen L. Johnson[1], Chris Wilson[4]

[1]Department of Earth Sciences, University of Oxford, Oxford, U.K.
[2]Department of Physical Oceanography, Woods Hole Oceanographic Institution, Woods Hole, MA, U.S.A
[3]Rosenstiel School of Marine, Atmospheric, and Earth Science, University of Miami, Miami, FL, U.S.A
[4]National Oceanography Centre, Liverpool, U.K.

Key Points:

- Water parcels recirculating in the subtropical gyre account for 37% of the total heat transport at 26.5°N in an eddy-rich ocean hindcast
- The heat transport of the subtropical gyre is associated with vertical overturning rather than the horizontal "gyre" circulation at 26.5°N
- Subtropical overturning plays a critical role in forming the source waters of the northward, subsurface limb of the Atlantic Meridional Overturning Circulation

Corresponding author: Oliver J. Tooth, oliver.tooth@seh.ox.ac.uk

Abstract

The Atlantic Meridional Overturning Circulation (AMOC) plays a critical role in the global climate system through the redistribution of heat, freshwater and carbon. At 26.5°N, the meridional heat transport has traditionally been partitioned geometrically into vertical and horizontal circulation contributions; however, attributing these components to the AMOC and Subtropical Gyre (STG) flow structures remains widely debated. Using water parcel trajectories evaluated within an eddy-rich ocean hindcast, we present the first Lagrangian decomposition of the meridional heat transport at 26.5°N. We find that water parcels recirculating within the STG account for 37% (0.36 PW) of the total heat transport across 26.5°N, more than twice that of the classical horizontal "gyre" component (15%). Rather than being distinct from the overturning circulation, the heat transport associated with the STG is due to the formation of subtropical mode waters via a shallow downward spiral, which ultimately feeds the northward limb of the AMOC.

Plain Language Summary

The Atlantic Meridional Overturning Circulation transports heat northward by converting warm, surface waters into cold waters returning at depth. In the subtropical North Atlantic, the heat transported by the overturning circulation has traditionally been separated from the wind-driven gyre circulation by assuming that the gyre flows horizontally along constant depth levels. By tracing the pathways of virtual water parcels in a high-resolution ocean model, we show that the heat transported by the subtropical gyre is larger than traditional estimates because water parcels spiral downwards across depth levels. Our results indicate that the subtropical gyre should not be considered separate from the overturning circulation, since the water parcels cooled within the gyre subsequently flow northwards to form cold waters in the subpolar North Atlantic.

1 Introduction

Throughout the coming century, the Atlantic Meridional Overturning Circulation (AMOC) will play a critical role in shaping the response of the global climate system to anthropogenic activity through the redistribution of excess heat, freshwater and carbon. Although there is strong consensus amongst coupled climate model projections that the AMOC will weaken during the 21st century (IPCC, 2021), scenario-based estimates of this weakening are wide-ranging across models and hence societally important impacts remain poorly constrained (e.g., Bellomo et al., 2021).

Central to the challenge of reducing uncertainty in future AMOC projections is the need to better understand historical ocean observations and their representation in numerical models. Since 2004, the Rapid Climate Change-Meridional Overturning Circulation and Heatflux Array (RAPID-MOCHA, herein referred to as RAPID) trans-basin observing system has made continuous measurements of the strength of the AMOC and the associated meridional transports of heat and freshwater across 26.5°N (Cunningham et al., 2007). Here, the subtropical North Atlantic Ocean transports $\sim$1.2 PW (1 PW $\equiv$ x10^{15} W) of heat northwards (Hall & Bryden, 1982; Johns et al., 2011; McCarthy et al., 2015a), accounting for 30% of the total ocean-atmosphere Meridional Heat Transport (MHT) (Ganachaud & Wunsch, 2000; Trenberth & Fasullo, 2017).

Traditionally, the total ocean heat transport across 26.5°N has been partitioned into zonally-averaged vertical and residual horizontal circulation components (Bryan, 1982; Böning & Herrmann, 1994; Johns et al., 2011), typically referred to as "overturning" and "gyre" heat transports, respectively. However, the degree to which these 2-dimensional geometric components represent the actual contributions made by the 3-dimensional flow structures of the AMOC and Subtropical Gyre (STG) to the total MHT at 26.5°N has been widely debated (e.g., Talley, 2003; Johns et al., 2023a). Previous studies have criticised this interpretation of the horizontal "gyre" circulation because the waters flowing northward within the western boundary current of the STG do not recirculate horizontally along constant depth surfaces, but rather spiral downwards to form Subtropical Mode Water (STMW) in a shallow overturning cell (Spall, 1992; Talley, 2003; Burkholder & Lozier, 2014; Berglund et al., 2022). According to Talley (2003), this wind-driven STMW cell within the STG could account for up to 0.4 PW of the total heat transport observed at 24°N, much larger than the traditional horizontal component of MHT. In contrast, the modelling study of Xu et al. (2016) concludes that the STG makes a negligible contribution to the total heat transport at 26.5°N since the authors argue that the near-surface waters of the Florida Current participate in the basin-wide AMOC rather than the STG circulation.

The long-standing uncertainty regarding the relative contributions of the AMOC and the STG flow structures to the total heat transport at 26.5°N ultimately reflects the subjective nature of approaching this problem within the confines of the traditional Eulerian framework (Johns et al., 2023a). To overcome this challenge, we present the first Lagrangian decomposition of the MHT and overturning across the RAPID 26.5°N array using water parcel trajectories evaluated within an eddy-rich ocean sea-ice hindcast simulation. We show that water parcels recirculating within the STG account for 37% (0.36 PW) of total MHT across 26.5°N between 2004-2015 while the remaining 63% (0.62 PW) is due to water parcels which continue northward to form NADW at subpolar latitudes. Further, our findings emphasise the important and historically-overlooked role of the STG in forming the source waters of the northward, subsurface limb of the AMOC.

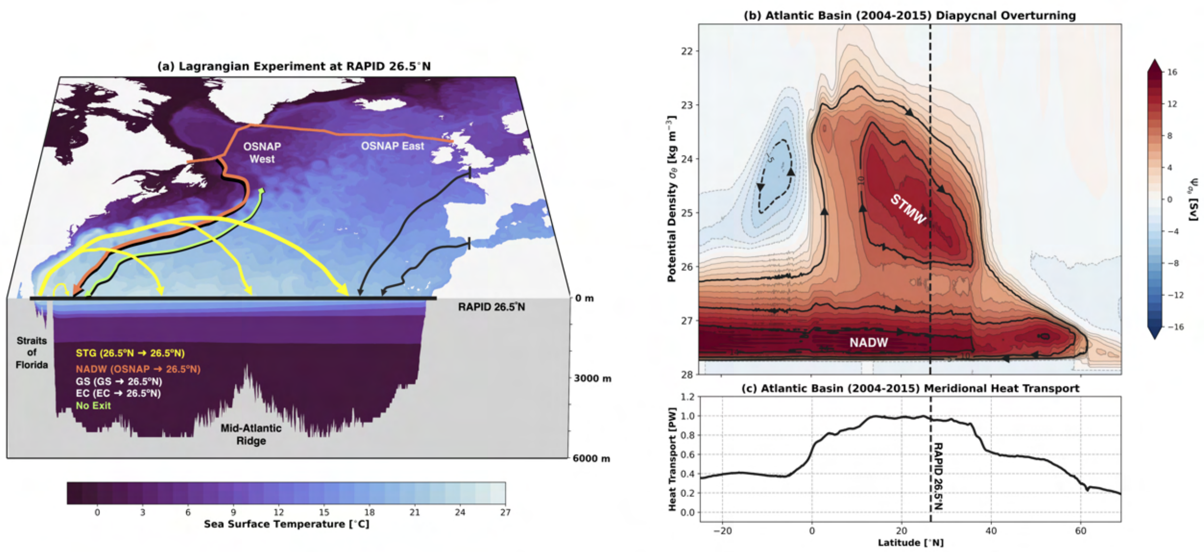

Figure 1. (a) Schematic representation of the Lagrangian pathways north of the RAPID array at 26.5°N. (b) Model time-mean Eulerian diapycnal overturning stream function calculated for the historical period 2004-2015. The contour interval is 1 Sv (1 Sv $\equiv$ 1x10^6 m^3 s^{-1}). Circulation is clockwise following positive (solid) streamlines and anti-clockwise following negative (dashed) streamlines. (c) Model time-mean Atlantic northward meridional heat transport as a function of latitude. The dashed black line denotes the location of the RAPID array at 26.5°N.

2 Materials and Methods

2.1 Ocean General Circulation Model

To investigate the meridional overturning and heat transport at 26.5°N, we use output from the ORCA0083-N06 ocean sea-ice hindcast simulation, documented in Moat et al. (2016). The simulation uses a global implementation of the Nucleus for European Modelling of the Ocean (NEMO) ocean circulation model version 3.6 (Madec, 2014) coupled to the Louvain-la-Neuve Ice Model version 2 (LIM2) sea-ice model (Bouillon et al., 2009). The ocean component is configured with a nominal horizontal resolution of 1/12° (equivalent to 8.3 km at 26.5°N) and with 75 unevenly spaced z-coordinate levels. The hindcast simulation is integrated for the historical period from 1958-2015 using the Drakkar Forcing Set 5.2 (Dussin et al., 2016). Here, we make use of the 5-day mean velocity and tracer fields output for the period 1980-2015.

Throughout this study, we compare the results derived from the ORCA0083-N06 simulation to observations made along the RAPID array at 26.5°N for the overlapping period 2004-2015 (Johns et al., 2023b). To ensure consistency between model and observational diagnostics, we implement a zero net volume transport constraint across 26.5°N, equivalent to that imposed by the RAPID program (e.g., Kanzow et al., 2010), in all Eulerian meridional overturning and heat transport calculations.

2.2 Lagrangian Particle Tracking

To determine the contributions of the STG and the large-scale overturning circulation to the total MHT at 26.5°N, we calculate the Lagrangian trajectories of virtual water parcels advected by the time-evolving velocity fields of the ORCA0083-N06 hindcast using TRACMASS version 7.1 (Aldama-Campino et al., 2020).

We initialise water parcels sampling the full-depth transport flowing southward across the RAPID 26.5°N section at the beginning of every month from 2004-2015. Water parcels are distributed in proportion to the southward transport across each grid cell face with a maximum volume transport of 0.005 Sv per parcel (1 Sv $\equiv$ 1x10^6 m^3 s^{-1}). Water parcels are advected backwards-in-time using the 5-day mean velocity fields for a maximum of 25 years to trace their origin. Water parcel trajectories are terminated on reaching this maximum advection time or when they meet any one of the following criteria: (i) recirculating back to the RAPID 26.5°N section, (ii) transiting to the Overturning in the Subpolar North Atlantic (OSNAP) array in the subpolar North Atlantic, or (iii) transiting to either the Gibraltar Strait or English Channel (Fig. 1a). Given that the advective timescales associated with the NADW cell have been found to be many decades longer than that of the STG (Tooth, Johnson, & Wilson, 2023; Petit et al., 2023), we consider only the subset of water parcels which return to 26.5°N within the STG in our analysis (see Text S1).

The location, conservative temperature and absolute salinity of each water parcel is recorded at every model grid cell crossing north of the RAPID 26.5°N section. The potential density referenced to the sea surface (σ_θ) is calculated along each trajectory using the TEOS-10 equation of state (McDougall et al., 2012) as implemented in the ORCA0083-N06 simulation.

2.3 Diagnosing Meridional Overturning and Heat Transport at 26.5°N

At subtropical latitudes, the meridional overturning has traditionally been defined in depth-space (Cunningham et al., 2007; Kanzow et al., 2010) since strong thermal stratification permits warm and saline water flowing northward to be vertically separated from its cold and fresh southward return flow (Kanzow et al., 2007). However, a notable disadvantage of calculating the overturning in-depth coordinates is that this does not distinguish between the distinct diapycnal overturning cells in the North Atlantic (Fig. 1b), namely, the lighter STMW cell and the denser NADW cell (Foukal & Chafik, 2022). We will therefore quantify the strength of the Eulerian overturning at 26.5°N by calculating meridional overturning streamfunctions in both depth (ψ_z) and density (ψ_{σ_θ}) coordinates after accounting for the net volume transport across the trans-basin section as follows:

$$\psi_z(z,t) = \int_z^0 \int_{x_w}^{x_e} v(x',z',t)\; dx'\; dz'$$

$$\psi_{\sigma_\theta}(\sigma_\theta,t) = \int_{x_w}^{x_e} \int_{z(x,\sigma_\theta,t)}^{0} v(x',z',t)\; dz'\; dx',$$

where $v(x,z,t)$ is the meridional velocity and $z(x,\sigma_\theta,t)$ is the time-evolving depth of the isopycnal σ_θ across the trans-basin section between the eastern (x_e) and western boundaries (x_w).

The northward MHT across 26.5°N is calculated following Moat et al. (2016) by integrating the product of the meridional velocity $v(x,z,t)$ and potential temperature (θ) over the full depth $H(x)$:

$$Q_{Total}(t) = \int_{-H(x)}^{0} \int_{x_w}^{x_e} \rho_o c_p\; v(x,z,t)\; \theta(x,z,t)\; dx\; dz$$

where the product of the seawater density and the specific heat capacity of seawater is given by $\rho_o c_p = 4.1\text{x}10^6$ J kg^{-1} °C^{-1} following Johns et al. (2011). We further partition the total MHT across the RAPID section Q_{Total} into horizontal "gyre" Q_{Gyre} and vertical "overturning" Q_{OT} (Bryden & Imawaki, 2001; Johns et al., 2011) components, as follows:

$$Q_{OT}(t) = \int_{-H}^{0} \int_{x_w}^{x_e} \rho_o c_p\; \langle v \rangle \langle \theta \rangle\; dx\; dz$$

$$Q_{Gyre}(t) = \int_{-H}^{0} \int_{x_w}^{x_e} \rho_o c_p\; v^*(x,z,t)\; \theta^*(x,z,t)\; dx\; dz$$

where $\langle v \rangle$ and $\langle \theta \rangle$ represent the zonally averaged velocity and potential temperature profiles (both functions of depth), and v^* and θ^* represent deviations from the zonally averaged profiles.

To complement the Eulerian diagnostics outlined above, we additionally quantify the strength of overturning and MHT across 26.5°N from the Lagrangian water parcel trajectories initialised between 2004-2015. To determine the vertical and diapycnal overturning taking place within the STG, we calculate partial Lagrangian overturning streamfunctions (Blanke et al., 1999; Döös et al., 2008) using only the water parcel trajectories which return to 26.5°N within the $\tau = 25$-year maximum advection period as follows (Tooth, Johnson, Wilson, & Evans, 2023):

$$F_z(z,t,\tau = 25\; yrs) = \int_z^0 V_{_{North}}(z,t-\tau) - V_{_{South}}(z,t)\; dz$$

$$F_{\sigma_\theta}(\sigma_\theta,t,\tau = 25\; yrs) = \int_{\sigma_\theta \geq \sigma'_\theta} V_{_{North}}(\sigma'_\theta,t-\tau) - V_{_{South}}(\sigma'_\theta,t)\; d\sigma'_\theta$$

where V_{North} and V_{South} represent the absolute volume transport distributions of all recirculating STG water parcels on their northward and southward crossings of the RAPID 26.5°N section.

Since Döös et al. (2008) showed that, provided a sufficiently large number of water parcels are initialised, the total Lagrangian overturning streamfunction will converge towards the time-mean Eulerian streamfunction, it follows that the time-mean overturning of the remaining NADW and AABW cells can be estimated by the residual $\overline{\psi_{\sigma_\theta}} - \overline{F_{\sigma_\theta}}$ (see Text S2).

We additionally define a Lagrangian measure of the net change in heat transport of the water parcels recirculating within the STG using their potential temperatures on their northward (θ_{North}) and southward (θ_{South}) crossings of the RAPID section at 26.5°N, $\Delta Q(t)$:

$$\Delta Q_{STG}(t, \tau = 25\ yrs) = \rho c_p \sum_{i=1}^{N} V_i \left(\theta_{North}(t-\tau) - \theta_{South}(t)\right)$$

where V_i is the volume transport conveyed by an individual water parcel i returning to 26.5°N, which is conserved along its Lagrangian trajectory.

3 Results

3.1 Evaluating Eulerian Meridional Overturning and Heat Transport at 26.5°N

We begin by adopting the traditional Eulerian frame of reference to compare the meridional overturning and heat transport simulated in ORCA0083-N06 to RAPID observations between 2004-2015. Although Figure 2a shows an overall agreement between the modelled and observed time-mean vertical overturning stream functions at 26.5°N, we find that the simulated 15.1 ± 2.8 Sv of vertical overturning is significantly weaker compared with observations (17.0 ± 3.6 Sv) and previous eddy-rich modelling studies (17.1 ± 2.6 Sv in Xu et al. (2016)).

Figures 2b-c present equivalent decompositions of the Eulerian heat transport across 26.5°N in both RAPID observations and the ORCA0083-N06 hindcast. Concordant with its weaker than observed overturning, the model time-mean MHT is 0.98 ± 0.21 PW compared with 1.2 ± 0.28 PW in observations. The model does, however, reproduce many features of the overturning and heat transport variability recorded in observations (Moat et al., 2016), including the reduction in overturning between 2009-2010 (McCarthy et al., 2012). Observations show that both the magnitude and variability of the MHT at 26.5°N is dominated ($> 90\%$) by the vertical "overturning" component, while $< 10\%$ is associated with the horizontal subtropical "gyre" component (Johns et al., 2011; McCarthy et al., 2015b; Johns et al., 2023a). Figure 2c shows a similar vertical-horizontal partition in ORCA0083-N06; the vertical cell accounts for 85% (0.84 ± 0.21 PW), and the horizontal cell for the remaining 15% of the total heat transport.

A closer examination of the simulated hydrography along 26.5°N shows that both the volume transport (31.3 ± 1.8 Sv) and temperature transport (2.56 ± 0.14 PW) of the Florida Current are well represented in the model compared with observed estimates reported in Meinen et al. (2010) and Johns et al. (2023a). Moat et al. (2016) instead highlighted the larger than observed southward Mid-Ocean (WB2 mooring to Africa) heat transport component in ORCA0083-N06 as the primary source of the model's underestimation of the observed total MHT. Further investigation indicates that, in the model, more of the warm and shallow waters transported northwards in the Florida Current are returned in the upper 100 m of the Mid-Ocean region along the RAPID array compared with observations (Fig. S2a). This is in contrast to previous studies, which have attributed the widespread underestimation of subtropical MHT in numerical models (e.g., Liu et al., 2022) to the overly diffusive thermocline simulated in z-coordinates (Msadek et al., 2013; Roberts et al., 2020), which results in a warmer than observed AMOC lower limb. Notably, there is good agreement between the basin-wide average potential temperature profiles simulated in ORCA0083-N06 and observed along the RAPID array (Fig. S2b), with even a slightly sharper main thermocline (between depths of 400-800m) in the model than in observations.

Since we propose that the excess shallow return flow in the STG accounts for the model's underestimation of vertical overturning (Fig. 2a) compared with observations at 26.5°N, it is informative to calculate a revised total MHT where an additional 1.9 Sv of northward transport is vertically overturned in accordance with observations. By assuming that this prematurely recirculated upper Florida Current water is instead returned to the RAPID section as NADW in the DWBC, we obtain a revised total MHT of 1.15 PW, in closer agreement with RAPID observations (see Text S3).

Overall, we find sufficient agreement between the structure and variability of both the vertical overturning and MHT simulated by ORCA0083-N06 and observations to justify our use of the model to better understand the contributions made by the STG and large-scale overturning circulation to the MHT at RAPID 26.5°N.

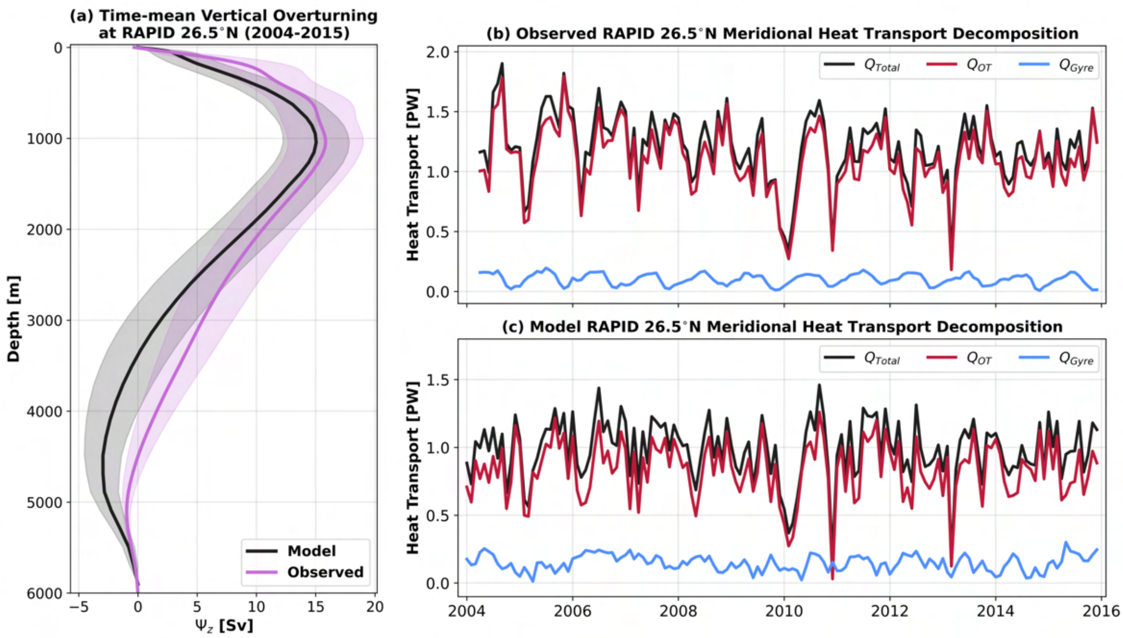

Figure 2. (a) Model (black) and observed (pink) time-mean (2004-2015) Eulerian vertical overturning stream functions calculated at RAPID 26.5°N. Shading denotes the standard deviation of the modelled and observed time-mean vertical overturning stream functions. (b) Total observed MHT (black) at 26.5°N decomposed into a zonally-averaged vertical "overturning" component (Q_{OT}, red) and a residual horizontal "gyre" component (Q_{Gyre}, blue). (c) As in (b) but calculated using model Eulerian meridional velocity and potential temperature fields at 26.5°N.

3.2 Lagrangian Decomposition of Meridional Overturning and Heat Transport at 26.5°N

To complement the classical Eulerian vertical-horizontal decomposition, we use our Lagrangian trajectories to quantify the contribution made by water parcels which recirculate in the STG to the time-mean heat transport at 26.5°N. We find that the STG circulation accounts for 0.36 ± 0.09 PW or 37 ± 9% of the total heat transport across 26.5°N in the model (Fig. 3a). This implies that the heat transport of the STG is more than twice that of the classical horizontal heat transport component and in closer agreement with the observed estimate of 0.4 PW at 24°N (Talley, 2003). Furthermore, Figure 3b confirms the assumption of Talley (2003) that the lightest waters flowing northward in the upper Florida Current ($\sigma_\theta < 25.875$) are returned across 26.5°N via the broad southward interior flow ($\sigma_\theta < 27.3$) between the Bahamas and Africa.

We additionally find that 83% of the STG heat transport is sourced from the upper 250 m of the Florida Current (Fig. S3). This contradicts the assumption made by Xu et al. (2016) that near-surface waters participate in the NADW cell and thus explains their substantial underestimation of the STG heat transport. Figure 3c shows that, on average, 4.8 Sv of the lightest waters transported in the Florida Current are vertically overturned within the STG, accounting for all of the Eulerian time-mean vertical overturning above 250 m at 26.5°N. Notably, while the STG circulation is found to contribute 1.6 Sv to the maximum overturning in depth-coordinates (z_{MOC_z} = 1045 m) in Figure 3c, we find that the entire STG heat transport can be accounted for by water parcels which return to 26.5°N within the AMOC upper limb (Fig. S3c). This implies that the volume flux across z_{MOC_z} within the STG is due to water parcels which return to 26.5°N along downwards sloping isotherms; i.e., without changing their temperature.

Although the strength of vertical overturning within the STG (4.8 Sv) broadly agrees with the magnitude of classical STMW formation (4.0 ± 1.0 Sv between θ = 17-19°C) north of 26.5°N, STMW explains less than a third (Fig. S3) of the total MHT of the STG. Diapycnal transformation within the STG instead peaks at lighter density classes ($\sigma_\theta <$ 26 kg m^{-3} in Fig. 3d) characteristic of Subtropical Underwater (STUW; O'Connor et al., 2005), which accounts for 47% of the STG heat transport (Fig. S3).

On classifying recirculating water parcels according to those which vertically overturn (which we here define as $|\Delta z| > 10$ m) and those which recirculate horizontally along approximately constant depth surfaces ($|\Delta z| \leq 10$ m), we find that both STG diapycnal overturning and MHT are dominated by water parcels which participate in the shallow vertical overturning cell (Fig. 3a). On the one hand, this is surprising since the large 6.7 Sv discrepancy between the strength of diapycnal and vertical overturning (Fig. 3c-d) in the STG suggests that a substantial component of gyre transport recirculates horizontally across sloping isopycnals at 26.5°N (Zhang & Thomas, 2021). However, further investigation reveals that this discrepancy is, in fact, due to both upwelling and downwelling water parcels undergoing substantial densification along-stream while compensating for one another in the depth-space overturning (see Fig. S4).

By subtracting the overturning associated with water parcels that recirculate in the STG from the Eulerian overturning streamfunctions in Figures 3c-d, we obtain an estimate for the contribution of the NADW cell to the total vertical and diapycnal overturning at 26.5°N. The residual vertical overturning streamfunction in Figure 3c (orange) shows that the upper limb of the NADW cell is sourced from waters flowing northward across the RAPID array between 200-1000 m depth. Furthermore, the positioning of the STMW cell and residual NADW cell in density-coordinates (Fig. 3d, 4a) confirms the earlier propositions of Burkholder and Lozier (2014) and Qu et al. (2013) that the mode waters returned in the southward limb of the shallow subtropical overturning cell are the principal source waters for the northward, subsurface limb of the NADW cell.

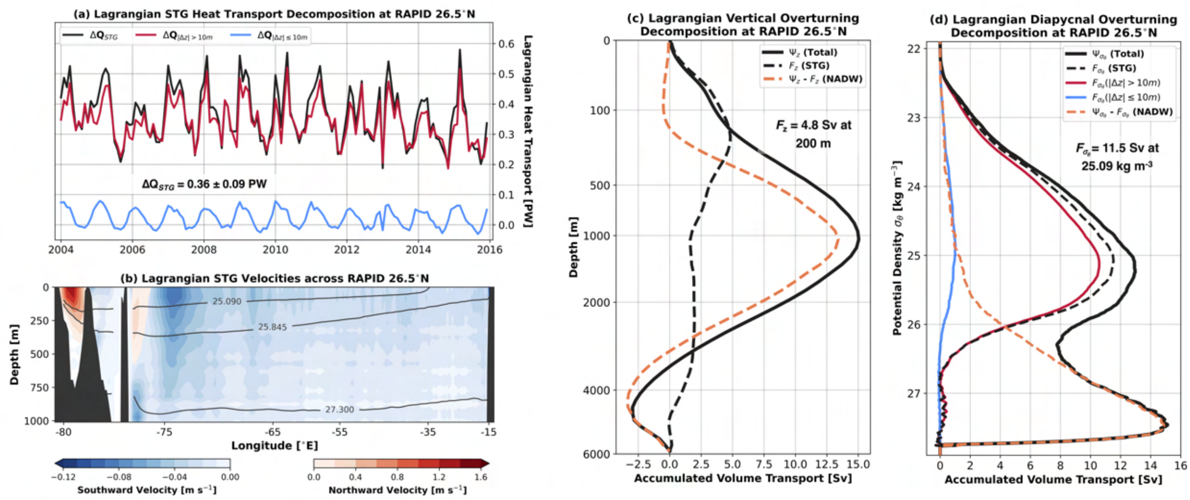

Figure 3. (a) Total Lagrangian heat transport of water parcels returning to 26.5°N in the STG (black) decomposed into the contributions of water parcels which vertically overturn ($|\Delta z|$ $>$ 10m, red) and those which recirculate horizontally along approximately constant isobaths ($|\Delta z|$ $\leq$ 10m, blue). (b) Distribution of STG water parcel northward (red contours) and southward (blue contours) crossings of the RAPID 26.5°N section shown here as an effective velocity in m s^{-1}. This is computed by summing the total volume transport through each model grid cell and normalising by the area. (c) Lagrangian decomposition of the time-mean (2004-2015) vertical overturning stream function at 26.5°N (Ψ_z, black solid) into a STG component (F_z, black dashed), determined from recirculating water parcel trajectories, and a residual NADW component (Ψ_z - F_z, orange dashed). (d) As in (c) for the time-mean diapycnal overturning stream function at 26.5°N. The STG diapycnal overturning component is further decomposed into the contributions of water parcels which vertically overturn (red) and those which recirculate horizontally (blue).

3.3 Redrawing the Meridional Overturning Circulation north of 26.5°N

We next interpret the findings of our Lagrangian analysis in the context of both RAPID observations and previous numerical modelling studies in order to revise the long-standing description of the AMOC north of 26.5°N. Following Burkholder and Lozier (2014), we seek to challenge the traditional conveyor-belt view of North Atlantic overturning, in which warm, surface waters are transported directly northward from subtropical to subpolar latitudes, where they are cooled by surface heat loss before returning southward at depth. We argue that both vertical and horizontal circulation cells are fundamental components of the AMOC and thus the large-scale overturning cannot be meaningfully distinguished from the gyre circulations of the North Atlantic. A more natural decomposition of the AMOC is between the STMW and NADW diapycnal overturning cells shown in Figure 4a since they capture the successive transformations required to form dense NADW from the lightest waters flowing northward in the upper Florida Current.

The wind-driven STMW cell is characterised by the formation of homogeneous, low potential vorticity (PV) mode water via intense wintertime surface buoyancy loss along the path of the Gulf Stream (e.g., Joyce et al., 2013). Constrained by the strong PV gradient across the subtropical basin (Bower et al., 1985; Lozier & Riser, 1990), mode waters are subducted below the seasonal thermocline when the upper ocean restratifies during spring (Kwon & Riser, 2004; Kwon et al., 2015) and thus imprint onto the vertical overturning rather than the horizontal circulation component. This subduction also marks the first of many downward cooling spirals (Spall, 1992) that mode waters must trace over the course of several decades (Berglund et al., 2022) within the STG in order to reach the depth ($z > 200$ m) and density ($\sigma_\theta > 25.5$ kg m^{-3}) required to be exported to subpolar latitudes. Our Lagrangian analysis indicates that, collectively, water parcels participating in the shallow subtropical overturning cell account for 37% of the MHT across 26.5°N. When applied to RAPID observations, this translates to 0.42 PW of the total 1.2 PW of MHT resulting from water mass transformation within the STG, which is in remarkable agreement with the 0.42 PW estimated by Johns et al. (2023a) when applying the approach of Talley (2003) to RAPID observations at 26.5°N.

In contrast to the STMW cell, the NADW cell spans both subtropical and subpolar latitudes (Fig. 4b), because the weaker PV gradient across the Gulf Stream at depth permits water parcels to be advected north-eastward via the subsurface pathways of the North Atlantic Current on sub-annual to inter-annual timescales (4 months - 7-years) (Jacobs et al., 2019; Burkholder & Lozier, 2011; Bower & Lozier, 1994; Gary et al., 2014). Since isopycnals shoal with latitude, subsurface water parcels will subsequently emerge as Subpolar Mode Water (SPMW) (Brambilla & Talley, 2006; de Boisséson et al., 2012) near the surface of the eastern subpolar gyre having been transformed by mixing with cooler, fresher recirculating subpolar waters (Berglund et al., 2023). An important implication of this subsurface subtropical to surface subpolar connectivity (Burkholder & Lozier, 2014) is that no inter-gyre pathway exists for sea surface temperature anomalies originating in the Gulf Stream to propagate advectively towards the eastern subpolar gyre (Foukal & Lozier, 2016). Figure 4a also highlights a central challenge of inferring large-scale circulation from Eulerian stream functions; the overturning streamfunction presented in Figure 1b misleadingly suggests a continuous meridional pathway from the lightest to the densest water masses in the North Atlantic while in fact there are two overlapping diapycnal cells.

On reaching subpolar latitudes, the NADW cell is more appropriately attributed to the horizontal circulation across sloping isopycnals rather than to a classical vertical overturning cell (Chafik & Rossby, 2019; Zhang & Thomas, 2021), and thus projects almost exclusively onto the overturning in density rather than depth-coordinates (Hirschi et al., 2020). Observations indicate that, on average, 17.0 ± 3.6 Sv of the water flowing northward across the RAPID array forms NADW through surface heat loss and mixing (Petit et al., 2020; Evans et al., 2023), which according to our Lagrangian analysis accounts for 63% or 0.78 PW of the total observed heat transport across 26.5°N.

4 Conclusions

In this study, we present the first Lagrangian decomposition of the meridional overturning and heat transport at 26.5°N using an eddy-rich ocean sea-ice hindcast. We draw three primary conclusions:

- The Lagrangian decomposition reveals that 37% (0.36 PW in ORCA0083-N06 or 0.42 PW when applied to RAPID observations) of the total MHT across 26.5°N is associated with the STG circulation.
- The downward spiralling nature of the STG circulation imprints onto the vertical "overturning" rather than horizontal "gyre" component of the time-mean MHT across 26.5°N.
- The shallow diapycnal overturning cell within the STG should be considered a fundamental component of the large-scale AMOC through its formation of STMW, which is subsequently transported northward in the subsurface layers of the AMOC's upper limb to participate in the formation of NADW.

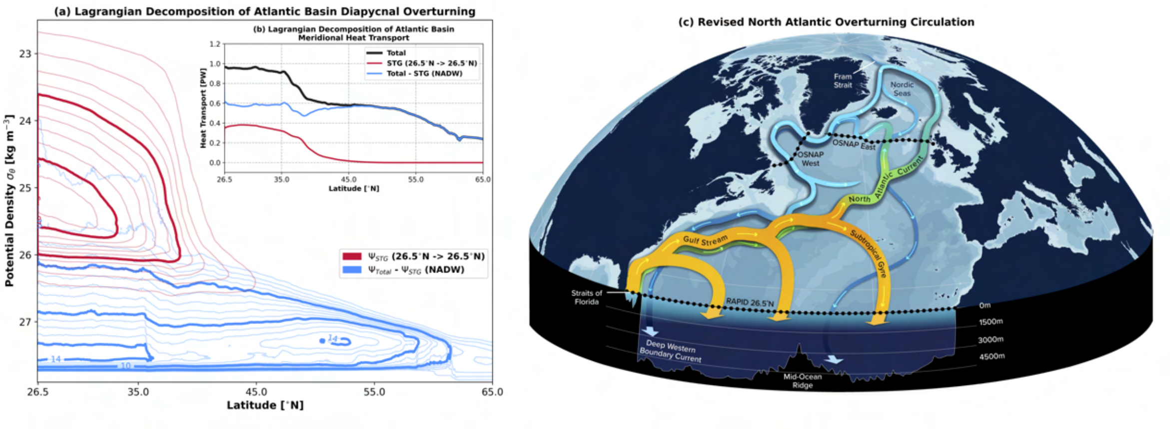

Figure 4. (a) Lagrangian decomposition of the time-mean (2004-2015) Atlantic Ocean diapycnal overturning stream function north of RAPID 26.5°N into a STG (STMW cell, red) component, derived from recirculating water parcel trajectories, and a residual component (NADW cell, blue). (b) Lagrangian decomposition of the latitudinal distribution of the time-mean Atlantic Ocean MHT (black) into the contributions of the STG circulation (STMW cell, red) and residual NADW cell (blue). (c) Schematic depicting the principal circulation components of the Atlantic Meridional Overturning Circulation (AMOC) north of the RAPID 26.5°N section.

Our study highlights that, in addition to their long-standing focus on the representation of NADW formation, numerical models need to adequately capture the circulation of the STMW cell in order to accurately represent both historical and future AMOC variability.

5 Open Research

The Lagrangian trajectory crossings of the RAPID 26.5°N section used in our analysis can be obtained from Tooth, Foukal, et al. (2023). The Lagrangian trajectory code TRACMASS was developed by Aldama-Campino et al. (2020). Data from the RAPID-MOCHA program are funded by the U.S. National Science Foundation and U.K. Natural Environment Research Council and are freely available to the public at https://www.rapid.ac.uk/rapidmoc and https://mocha.rsmas.miami.edu/mocha. The specific version of the observed RAPID-MOCHA heat transport data used in this study is Johns et al. (2023b).

Acknowledgments

O.J. Tooth is grateful for the financial support of the UK Natural Environment Research Council (NE/S007474/1). N.P. Foukal was supported by the Andrew W. Mellon Foundation Endowed Fund for Innovative Research from the Woods Hole Oceanographic Institution. W.E. Johns was supported by the grants OCE-1926008 and OCE-2148723 from the U.S. National Science Foundation. H.L. Johnson was supported by the NERC-NSF grant SNAP-DRAGON (NE/T013494/1). C.W. was jointly supported by the NERC LTS-S CLASS (Climate-Linked Atlantic Sector Science) grant (NE/R015953/1) and the NERC LTS-M CANARI (Climate change in the Arctic-North Atlantic Region and Impacts on the UK) grant (NE/W004984/1).

References

Aldama-Campino, A., Döös, K., Kjellsson, J., & Jönsson, B. (2020). *TRACMASS: Formal release of version 7.0 (v7.0-beta). Zenodo.* doi: 10.5281/zenodo.4337926

Bellomo, K., Angeloni, M., Corti, S., & von Hardenberg, J. (2021). Future climate change shaped by inter-model differences in atlantic meridional overturning circulation response. *Nature Communications*, *12*(1), 3659. doi: 10.1038/s41467-021-24015-w

Berglund, S., Döös, K., Groeskamp, S., & McDougall, T. (2023). North Atlantic Ocean circulation and related exchange of heat and salt between water masses. *Geophysical Research Letters*, *50*(e2022GL100989). doi: 10.1029/2022GL100989

Berglund, S., Döös, K., Groeskamp, S., & McDougall, T. J. (2022, April). The downward spiralling nature of the North Atlantic Subtropical Gyre. *Nature Communications*, *13*(1), 2000. doi: 10.1038/s41467-022-29607-8

Blanke, B., Arhan, M., Madec, G., & Roche, S. (1999). Warm Water Paths in the Equatorial Atlantic as Diagnosed with a General Circulation Model. *Journal of Physical Oceanography*, *29*(11), 2753 – 2768. (Place: Boston MA, USA Publisher: American Meteorological Society) doi: https://doi.org/10.1175/1520-0485(1999)029⟨2753:WWPITE⟩2.0.CO;2

Bouillon, S., Ángel Morales Maqueda, M., Legat, V., & Fichefet, T. (2009). An elastic–viscous–plastic sea ice model formulated on arakawa b and c grids. *Ocean Modelling*, *27*(3), 174-184. doi: https://doi.org/10.1016/j.ocemod.2009.01.004

Bower, A., & Lozier, M. (1994). A closer look at particle exchange in the gulf stream. *J. Phys. Oceanogr.*, *24*, 1399–1418.

Bower, A., Rossby, H., & Lillibridge, J. (1985). The Gulf Stream—Barrier or Blender? *Journal of Physical Oceanography*, *15*(1), 24 – 32. (Place: Boston MA, USA Publisher: American Meteorological Society) doi: https://doi.org/10.1175/1520-0485(1985)015⟨0024:TGSOB⟩2.0.CO;2

Brambilla, E., & Talley, L. (2006). Surface drifter exchange between the north atlantic subtropical and subpolar gyres. *Journal of Geophysical Research*, *111*. doi: 10.1029/2005JC003146

Bryan, K. (1982). Seasonal variation in meridional overturning and poleward heat transport in the atlantic and pacific oceans: A model study. *J. Mar. Res.*, *40*, 39-53.

Bryden, H., & Imawaki, S. (2001). Ocean heat transport [Book Section]. In G. Siedler, J. Church, & J. Gould (Eds.), *Ocean circulation and climate: Observing and modelling the global ocean* (p. 455-474). International Geophysics Series No. 77. Academic Press.

Burkholder, K. C., & Lozier, M. S. (2011). Subtropical to subpolar pathways in the North Atlantic: Deductions from Lagrangian trajectories. *Journal of Geophysical Research: Oceans*, *116*(C7). (_eprint: https://agupubs.onlinelibrary.wiley.com/doi/pdf/10.1029/2010JC006697) doi: https://doi.org/10.1029/2010JC006697

Burkholder, K. C., & Lozier, M. S. (2014). Tracing the pathways of the upper limb of the north atlantic meridional overturning circulation. *Geophysical Research Letters*, *41*(12), 4254–4260. (_eprint: https://agupubs.onlinelibrary.wiley.com/doi/pdf/10.1002/2014GL060226) doi: https://doi.org/10.1002/2014GL060226

Böning, C. W., & Herrmann, P. (1994). Annual Cycle of Poleward Heat Transport in the Ocean: Results from High-Resolution Modeling of the North and Equatorial Atlantic. *Journal of Physical Oceanography*, *24*(1), 91 – 107. (Place: Boston MA, USA Publisher: American Meteorological Society) doi: https://doi.org/10.1175/1520-0485(1994)024⟨0091:ACOPHT⟩2.0.CO;2

Chafik, L., & Rossby, T. (2019). Volume, Heat, and Freshwater Divergences in the Subpolar North Atlantic Suggest the Nordic Seas as Key to the State of the Meridional Overturning Circulation. *Geophysical Research Letters*, *46*(9), 4799–4808. doi: 10.1029/2019GL082110

Cunningham, S., Kanzow, T., Rayner, D., Baringer, M., Johns, W., Marotzke, J., ... Bryden, H. (2007, Aug). Temporal Variability of the Atlantic Meridional Overturning Circulation at 26.5°N. *Science*, *317*(5840), 935–938. (American Association for the Advancement of Science) doi: 10.1126/science.1141304

de Boisséson, E., Thierry, V., Mercier, H., Caniaux, G., & Desbruyères, D. (2012). Origin, formation and variability of the Subpolar Mode Water located over the Reykjanes Ridge. *Journal of Geophysical Research: Oceans*, *117*. doi: 10.1029/2011jc007519

Dussin, R., Barnier, B., Brodeau, L., & Molines, J. M. (2016). *The making of the DRAKKAR forcing set DFS5* (Tech. Rep.). Retrieved from `https://www.drakkar-ocean.eu/publications/reports/report{\_}DFS5v3{\_}April2016.pdf`

Döös, K., Nycander, J., & Coward, A. C. (2008). Lagrangian decomposition of the Deacon Cell. *Journal of Geophysical Research: Oceans*, *113*(C7). (_eprint: https://agupubs.onlinelibrary.wiley.com/doi/pdf/10.1029/2007JC004351) doi: https://doi.org/10.1029/2007JC004351

Evans, D. G., Holliday, N. P., Bacon, S., & Le Bras, I. (2023). Mixing and air–sea buoyancy fluxes set the time-mean overturning circulation in the subpolar North Atlantic and Nordic Seas. *Ocean Science*, *19*(3), 745–768. doi: 10.5194/os-19-745-2023

Foukal, N., & Chafik, L. (2022). The amoc needs a universally-accepted definition. *Authorea*. doi: 10.1002/essoar.10512765.1

Foukal, N., & Lozier, M. (2016). No inter-gyre pathway for sea-surface temperature anomalies in the north atlantic. *Nature Communications*, *7*. doi: 10.1038/ncomms11333

Ganachaud, A., & Wunsch, C. (2000). Improved estimates of global ocean circulation, heat transport and mixing from hydrographic data. *Nature*, *408*(6811), 453–457. doi: https://doi.org/10.1038/35044048

Gary, S., Lozier, M., Kwon, Y., & Park, J. (2014). The fate of north atlantic subtropical mode water in the flame model. *J. Phys. Oceanogr.*, *44*, 1354 – 1371. doi: 10.1175/JPO-D-13-0202.1

Hall, M., & Bryden, H. (1982). Direct estimates and mechanisms of ocean heat transport. *Deep Sea Res.*(29), 339-359.

Hirschi, J. J.-M., Barnier, B., Böning, C., Biastoch, A., Blaker, A. T., Coward, A., ... Xu, X. (2020). The atlantic meridional overturning circulation in high-resolution models. *Journal of Geophysical Research: Oceans*, *125*(4), e2019JC015522. doi: https://doi.org/10.1029/2019JC015522

IPCC. (2021). Summary for policymakers [Book Section]. In V. Masson-Delmotte et al. (Eds.), *Climate change 2021: The physical science basis. contribution of working group i to the sixth assessment report of the intergovernmental panel on climate change* (p. 332). Cambridge, United Kingdom and New York, NY, USA: Cambridge University Press. doi: 10.1017/9781009157896.001

Jacobs, Z. L., Grist, J. P., Marsh, R., & Josey, S. A. (2019). A Subannual Subsurface Pathway From the Gulf Stream to the Subpolar Gyre and Its Role in Warming and Salinification in the 1990s. *Geophysical Research Letters*, *46*(13), 7518–7526. (_eprint: https://agupubs.onlinelibrary.wiley.com/doi/pdf/10.1029/2019GL083021) doi: https://doi.org/10.1029/2019GL083021

Johns, W., Baringer, M., Beal, L., Cunningham, S., Kanzow, T., Bryden, H., ... Curry, R. (2011). Continuous, Array-Based Estimates of Atlantic Ocean Heat Transport at 26.5°N. *Journal of Climate*, *24*(10), 2429 – 2449. (Place: Boston MA, USA Publisher: American Meteorological Society) doi:

https://doi.org/10.1175/2010JCLI3997.1

Johns, W., Elipot, S., Smeed, D., Moat, B., King, B., Volkov, D., & Smith, R. (2023a). Towards two decades of atlantic ocean mass and heat transports at 26.5°N. *Philosophical Transactions of the Royal Society A: Mathematical, Physical and Engineering Sciences*, *381*(2262), 20220188. doi: 10.1098/rsta.2022.0188

Johns, W., Elipot, S., Smeed, D., Moat, B., King, B., Volkov, D., & Smith, R. (2023b). *(v.2020) Atlantic Meridional Overturning Circulation (AMOC) Heat Transport Time Series between April 2004 and December 2020 at 26.5°N* [dataset]. University of Miami Libraries. doi: https://doi.org/10.17604/3nfq-va20

Joyce, T. M., Thomas, L. N., Dewar, W. K., & Girton, J. B. (2013). Eighteen degree water formation within the gulf stream during climode. *Deep Sea Research Part II: Topical Studies in Oceanography*, *91*, 1-10. (Subtropical Mode Water in the North Atlantic Ocean) doi: https://doi.org/10.1016/j.dsr2.2013.02.019

Kanzow, T., Cunningham, S. A., Johns, W. E., Hirschi, J. J.-M., Marotzke, J., Baringer, M. O., … Collins, J. (2010). Seasonal variability of the atlantic meridional overturning circulation at 26.5°n. *Journal of Climate*, *23*(21), 5678 - 5698. doi: 10.1175/2010JCLI3389.1

Kanzow, T., Cunningham, S. A., Rayner, D., Hirschi, J. J.-M., Johns, W. E., Baringer, M. O., … Marotzke, J. (2007, August). Observed Flow Compensation Associated with the MOC at 26.5°N in the Atlantic. *Science*, *317*(5840), 938–941. (Publisher: American Association for the Advancement of Science) doi: 10.1126/science.1141293

Kwon, Y., Park, J., Gary, S. F., & Lozier, M. (2015). Year-to-year reoutcropping of eighteen degree water in an eddy-resolving ocean simulation. *J. Phys. Oceanogr.*, *45*, 1189–1204. doi: 10.1175/JPO-D-14-0122.1.

Kwon, Y., & Riser, S. (2004). North atlantic subtropical mode water: A history of ocean-atmosphere interaction 1961–2000. *Geophys. Res. Lett.*, *31*. doi: 10.1029/2004GL021116

Liu, C., Yang, Y., Liao, X., Cao, N., Liu, J., Ou, N., … Zheng, R. (2022, November). Discrepancies in Simulated Ocean Net Surface Heat Fluxes over the North Atlantic. *Advances in Atmospheric Sciences*, *39*(11), 1941–1955. doi: 10.1007/s00376-022-1360-7

Lozier, M. S., & Riser, S. C. (1990). Potential Vorticity Sources and Sinks in a Quasi-geostrophic Ocean: beyond Western Boundary Currents. *Journal of Physical Oceanography*, *20*(10), 1608 – 1627. (Place: Boston MA, USA Publisher: American Meteorological Society) doi: https://doi.org/10.1175/1520-0485(1990)020⟨1608:PVSASI⟩2.0.CO;2

Madec, G. (2014). *NEMO Ocean Engine. Note du Pôle Modélisation de l'Institut Pierre-Simon Laplace 27* (Tech. Rep.).

McCarthy, G., Frajka-Williams, E., Johns, W., Baringer, M., Meinen, C., Bryden, H., … Cunningham, S. (2012). Observed interannual variability of the Atlantic meridional overturning circulation at 26.5°N. *Geophysical Research Letters*, *39*(19). doi: https://doi.org/10.1029/2012GL052933

McCarthy, G., Smeed, D., Johns, W., Frajka-Williams, E., Moat, B., Rayner, D., … Bryden, H. (2015a). Measuring the atlantic meridional overturning circulation at 26°n. *Progress in Oceanography*, *130*, 91-111. doi: https://doi.org/10.1016/j.pocean.2014.10.006

McCarthy, G., Smeed, D., Johns, W., Frajka-Williams, E., Moat, B., Rayner, D., … Bryden, H. (2015b). Measuring the Atlantic Meridional Overturning Circulation at 26°N. *Progress in Oceanography*, *130*, 91–111. doi: https://doi.org/10.1016/j.pocean.2014.10.006

McDougall, T. J., Jackett, D. R., Millero, F. J., Pawlowicz, R., & Barker, P. M. (2012). A global algorithm for estimating Absolute Salinity. *Ocean Science*, *8*(6), 1123–1134. doi: 10.5194/os-8-1123-2012

Meinen, C. S., Baringer, M. O., & Garcia, R. F. (2010). Florida Current transport variability: An analysis of annual and longer-period signals. *Deep Sea Research Part I: Oceanographic Research Papers*, *57*(7), 835–846. doi: https://doi.org/10.1016/j.dsr.2010.04.001

Moat, B. I., Josey, S. A., Sinha, B., Blaker, A. T., Smeed, D. A., McCarthy, G. D., ... Coward, A. C. (2016). Major variations in subtropical North Atlantic heat transport at short (5 day) timescales and their causes. *Journal of Geophysical Research: Oceans*, *121*(5), 3237–3249. (_eprint: https://agupubs.onlinelibrary.wiley.com/doi/pdf/10.1002/2016JC011660) doi: https://doi.org/10.1002/2016JC011660

Msadek, R., Johns, W. E., Yeager, S. G., Danabasoglu, G., Delworth, T. L., & Rosati, A. (2013). The Atlantic Meridional Heat Transport at 26.5°N and Its Relationship with the MOC in the RAPID Array and the GFDL and NCAR Coupled Models. *Journal of Climate*, *26*(12), 4335 – 4356. (Place: Boston MA, USA Publisher: American Meteorological Society) doi: https://doi.org/10.1175/JCLI-D-12-00081.1

O'Connor, B. M., Fine, R. A., & Olson, D. B. (2005). A global comparison of subtropical underwater formation rates. *Deep Sea Research Part I: Oceanographic Research Papers*, *52*(9), 1569-1590. doi: https://doi.org/10.1016/j.dsr.2005.01.011

Petit, T., Lozier, M. S., Josey, S. A., & Cunningham, S. A. (2020, nov). Atlantic Deep Water Formation Occurs Primarily in the Iceland Basin and Irminger Sea by Local Buoyancy Forcing. *Geophysical Research Letters*, *47*(22). doi: 10.1029/2020GL091028

Petit, T., Lozier, M. S., Rühs, S., Handmann, P., & Biastoch, A. (2023). Propagation and Transformation of Upper North Atlantic Deep Water From the Subpolar Gyre to 26.5°N. *Journal of Geophysical Research: Oceans*, *128*(8), e2023JC019726. (_eprint: https://agupubs.onlinelibrary.wiley.com/doi/pdf/10.1029/2023JC019726) doi: https://doi.org/10.1029/2023JC019726

Qu, T., Gao, S., & Fukumori, I. (2013). Formation of salinity maximum water and its contribution to the overturning circulation in the north atlantic as revealed by a global general circulation model. *Journal of Geophysical Research: Oceans*, *118*(4), 1982-1994. doi: https://doi.org/10.1002/jgrc.20152

Roberts, M. J., Jackson, L. C., Roberts, C. D., Meccia, V., Docquier, D., Koenigk, T., ... Wu, L. (2020). Sensitivity of the Atlantic Meridional Overturning Circulation to Model Resolution in CMIP6 HighResMIP Simulations and Implications for Future Changes. *Journal of Advances in Modeling Earth Systems*, *12*(8), e2019MS002014. (_eprint: https://agupubs.onlinelibrary.wiley.com/doi/pdf/10.1029/2019MS002014) doi: https://doi.org/10.1029/2019MS002014

Spall, M. A. (1992). Cooling Spirals and Recirculation in the Subtropical Gyre. *Journal of Physical Oceanography*, *22*(5), 564 – 571. (Place: Boston MA, USA Publisher: American Meteorological Society) doi: https://doi.org/10.1175/1520-0485(1992)022⟨0564:CSARIT⟩2.0.CO;2

Talley, L. D. (2003). Shallow, Intermediate, and Deep Overturning Components of the Global Heat Budget. *Journal of Physical Oceanography*, *33*(3), 530–560. doi: 10.1175/1520-0485(2003)033⟨0530:SIADOC⟩2.0.CO;2

Tooth, O., Foukal, N., Johns, W., Johnson, H., & Wilson, C. (2023). *Lagrangian decomposition of the meridional heat transport at 26.5n water parcel crossings of the rapid 26.5n array* [dataset]. Zenodo. doi: https://doi.org/10.5281/zenodo.10069800

Tooth, O., Johnson, H., & Wilson, C. (2023). Lagrangian overturning pathways in the eastern subpolar north atlantic. *Journal of Climate*, *36*(3), 823 - 844. doi:

10.1175/JCLI-D-21-0985.1

Tooth, O., Johnson, H., Wilson, C., & Evans, D. (2023). Seasonal overturning variability in the eastern north atlantic subpolar gyre: a lagrangian perspective. *Ocean Science*, *19*(3), 769–791. doi: 10.5194/os-19-769-2023

Trenberth, K. E., & Fasullo, J. T. (2017). Atlantic meridional heat transports computed from balancing Earth's energy locally. *Geophysical Research Letters*, *44*(4), 1919–1927. (_eprint: https://agupubs.onlinelibrary.wiley.com/doi/pdf/10.1002/2016GL072475) doi: https://doi.org/10.1002/2016GL072475

Xu, X., Rhines, P. B., & Chassignet, E. P. (2016). Temperature–Salinity Structure of the North Atlantic Circulation and Associated Heat and Freshwater Transports. *Journal of Climate*, *29*(21), 7723 – 7742. (Place: Boston MA, USA Publisher: American Meteorological Society) doi: https://doi.org/10.1175/JCLI-D-15-0798.1

Zhang, R., & Thomas, M. (2021). Horizontal circulation across density surfaces contributes substantially to the long-term mean northern Atlantic Meridional Overturning Circulation. *Communications Earth & Environment*, *2*(1). doi: 10.1038/s43247-021-00182-y

Supporting Information for "Lagrangian Decomposition of the Meridional Heat Transport at 26.5°N"

Oliver J. Tooth[1], Nicholas P. Foukal[2], William E. Johns[3], Helen L. Johnson[1], Chris Wilson[4]

[1]Department of Earth Sciences, University of Oxford, Oxford, U.K.

[2]Department of Physical Oceanography, Woods Hole Oceanographic Institution, Woods Hole, MA, U.S.A

[3]Rosenstiel School of Marine, Atmospheric, and Earth Science, University of Miami, Miami, FL, U.S.A

[4]National Oceanography Centre, Liverpool, U.K.

Contents of this file

1. Text S1 to S3
2. Figures S1 to S4
3. Table T1

Introduction Here we provide additional details on the Lagrangian particle tracking experiments and construction of the Lagrangian overturning streamfunctions discussed in the manuscript. Section S1 further describes the backwards-in-time Lagrangian particle tracking experiments undertaken at the RAPID 26.5°N section in the ORCA0083-N06 ocean sea-ice hindcast. Section S2 outlines the methodology used to construct Lagrangian overturning streamfunctions from the water parcel trajectories evaluated in this study. Section S3 describes how we obtained a revised estimate for the total meridional heat transport at 26.5°N by accounting for the weaker-than-observed vertical overturning in the ORCA0083-N06 hindcast.

Text S1.

Further information on the backwards-in-time Lagrangian particle tracking experiments undertaken at RAPID 26.5°N in ORCA0083-N06.

To evaluate the Lagrangian trajectories of water parcels released along the RAPID section at 26.5°N in the ORCA0083-N06 ocean sea-ice hindcast, we used the Lagrangian particle tracking tool TRACMASS v7.1 (Aldama-Campino et al., 2020). TRACMASS uses a mass conserving scheme which determines the trajectory path of each water parcel analytically by solving a differential equation for the unique streamlines of the flow in each model grid cell (Döös et al., 2008). We chose to use the stepwise stationary scheme, which divides the time between successive 5-day mean velocity fields into a series of 100 intermediate time steps. The velocity field at each intermediate time step is determined by linear interpolation and is assumed to be steady for the duration of the step (Döös et al., 2017). Since ORCA0083-N06 uses a Boussinesq ocean circulation model (Nucleus for European Modelling of the Ocean [NEMO] version 3.6), the volume transport conveyed by each water parcel is conserved along its entire trajectory. To ensure mass is conserved within each model grid cell, we did not choose to parameterise sub-grid scale convective mixing along water parcel trajectories. This enables us to advect water parcels backwards-in-time and construct partial Lagrangian streamfunctions from their trajectories (see Text

S2.). For further details of TRACMASS and its associated trajectory schemes, readers are referred to Döös et al. (2017).

Over the course of our Lagrangian experiment, a total of 12.3 million water parcels were initialised to sample the full-depth southward transport across the RAPID section over 144 successive months between January 2004 and December 2015. Water parcels were initialised on the earliest available day of each month based on the centre of the nearest 5-day mean window in the ORCA0083-N06 hindcast. We chose to evaluate backwards-in-time water parcel trajectories in order to produce Lagrangian diagnostics for the period overlapping the continuous heat and mass transport observations made at RAPID 26.5°N (2004-2015). Since water parcels are advected through the 3-dimensional flow field for a maximum of 25 years, our Lagrangian experiment uses model velocity and tracer fields for the extended period 1980-2015. As outlined in the main text, water parcel trajectories are terminated on meeting any one of the following criteria: (i) recirculating back to the RAPID 26.5°N section, (ii) reaching the Overturning in the Subpolar North Atlantic (OSNAP) array in the subpolar North Atlantic, or (iii) reaching either the Gibraltar Strait or the English Channel. Table **T1** presents a decomposition of the origins of the time-mean volume transport flowing southward across the RAPID section. The overwhelming majority of the southward transport at 26.5°N (91.3%) originates from 26.5°N and thus represents subtropical gyre recirculation. Furthermore, Figure S1 shows that the 25-year maximum advection time is sufficient to fully resolve the subtropical gyre circulation since the accumulated volume transport returning to the RAPID section has stabilised within this period. The 15.29 Sv of volume transport which remains within our subtropical

North Atlantic domain following 25 years of advection is therefore not considered to be part of the subtropical gyre circulation, but rather a combination of slowly transiting North Atlantic Deep Water (NADW) and water parcels continuously circulating at depth within our domain.

Text S2.

Further information on the definition of Lagrangian overturning streamfunctions and their use to decompose the time-mean Eulerian overturning at RAPID 26.5°N.

To compute the vertical Lagrangian overturning from the backwards-in-time trajectories initialised at time t, we first determine the absolute volume transport distributions of all water parcels recirculating within the subtropical gyre in discrete depth bins on their initial southward V_{South} and final northward V_{North} crossings of the RAPID 26.5°N section. We then calculate the Lagrangian overturning streamfunction F_z in-depth coordinates as the cumulative sum of the net volume transport distribution from the seafloor to the ocean surface as follows:

$$F_z(z, t, \tau = 25\ yrs) = \int_z^0 V_{North}(z, t - \tau) - V_{South}(z, t)\ dz$$

Similarly, the diapycnal Lagrangian overturning streamfunction F_{σ_θ} can be computed by accumulating the net volume transport distribution of recirculating water parcels in potential density coordinates:

$$F_{\sigma_\theta}(\sigma_\theta, t, \tau = 25\ yrs) = \int_{\sigma_\theta \geq \sigma'_\theta} V_{North}(\sigma'_\theta, t - \tau) - V_{South}(\sigma'_\theta, t)\ d\sigma'_\theta$$

The equations outlined above, defined as Lagrangian overturning functions in Tooth, Johnson, Wilson, and Evans (2023), are, in fact, a specific case of the more general Lagrangian meridional overturning streamfunctions first introduced by Blanke, Arhan, Madec, and Roche (1999). Blanke et al. (1999) showed that, for a given collection of water parcels flowing from an initial section to a final section, the Lagrangian meridional overturning streamfunctions $\Psi_{j,k}$ ($\Psi_{j,\sigma}$) in depth (potential density) coordinates is given by:

$$\Psi_{j,k} = \sum_{k_{min}}^{k} \sum_{i} \sum_{n} V^{y}_{i,j,k,n}$$

$$\Psi_{j,\sigma} = \sum_{\sigma_{min}}^{\sigma} \sum_{i} \sum_{n} V^{y}_{i,j,\sigma,n}$$

where i, j and k are the zonal, meridional and vertical indices of the discretised model grid and σ represents a discrete potential density space. $V_{i,j,k,n}$ is the volume transport of a water parcel n crossing a line of constant latitude y.

An important property of the Lagrangian meridional overturning streamfunctions defined above is that, provided a sufficient number of water parcel trajectories are initialised from the chosen section, Döös et al. (2008) showed that $\Psi_{j,k}$ and $\Psi_{j,\sigma}$ will converge towards their equivalent time-mean Eulerian streamfunctions. Thus, since we fully resolve the subtropical circulation within our Lagrangian experiment, we can estimate the contributions made by the outstanding NADW and Antarctic Bottom Water trajectories to the total Eulerian overturning streamfunction by calculating the residual between the time-mean Eulerian quantity and the Lagrangian overturning streamfunction for the subtropical gyre circulation (i.e., $\overline{\psi}(y, \sigma_\theta) - \overline{\Psi}^{STG}_{j,\sigma_\theta}$).

Text S3.

Further information on calculating a revised estimate of the meridional heat transport across 26.5°N in ORCA0083-N06.

The total meridional heat transport across 26.5°N is 0.98 ± 0.21 PW in ORCA0083-N06 compared with 1.20 ± 0.28 PW in RAPID observations (2004-2015). To better understand the reason for the model's weaker total heat transport across 26.5°N compared with observations, we first examined the volume and temperature transports of the Florida Current to assess whether the model simulates a sufficient flux of the northward flowing warm water compared with observations. As previously discussed by Moat et al. (2016), the ORCA0083-N06 hindcast does adequately represent both the volume transport (31.3 ± 1.8 Sv) and temperature transport (2.56 ± 0.14 PW) of the Florida Current when compared with observations (Meinen et al., 2010; ?, ?). Instead, we identify the shallow return flow in the upper Mid-Ocean (RAPID WB2 mooring to Africa) as the principal source of the model's weaker total heat transport compared with observations. This is shown in Figure S2 where, despite good agreement being found between the simulated and observed mean potential temperature profiles for the Mid-Ocean region, there is clearly greater southward volume transport in the upper 150 m in the model compared with RAPID observations.

A closer examination of the zonal distribution of southward subtropical gyre transport between WB2 and Africa (see Fig. S4a) indicates that the southward flow is especially concentrated in the upper 150 m between -75.5°E and -72°E where potential temperatures, on average, exceed 23°C (see Fig. S3a). Furthermore, Figure S3b shows that water flowing southward across the RAPID section in this potential temperature range ($\theta > 23°$C) contributes negligibly to the time-mean meridional heat transport of the subtropical gyre circulation, given that isotherms do not slope significantly in this region when averaged on longer than seasonal timescales (see Fig. S3a). By extension, this also implies that the greater shallow return flow does not contribute to the model's total heat transport of 0.98 ± 0.21 PW across 26.5°N. However, by comparing the observed and simulated vertical overturning at 26.5°N, we do know that the model underestimates the strength of meridional overturning by 1.9 Sv (17.0 Sv - 15.1 Sv) compared with RAPID observations from 2004-2015. Thus, we can estimate a revised total heat transport at 26.5°N by assuming that a further 1.9 Sv of northward transport flowing across the RAPID section is vertically overturned and returns as NADW in the Deep Western Boundary Current in accordance with observations. To do this, we first need to quantify the surplus meridional heat transport, Q_s, due to the larger net change in potential temperature ($\Delta\theta$) of the recirculating volume transport ($V = 1.9$ Sv) absent from the model's meridional overturning circulation:

$$Q_s = \rho_0 C_p V \Delta\theta = 0.17\ PW$$

where $\rho_0 C_p = 4.1\text{x}10^6$ J kg^{-1} C^{-1} following Johns et al. (2011) and $\Delta\theta = \theta_{North} - \theta_{South} =$ 26°C - 4.5°C. Here, we have chosen $\theta_{North} = 26°$C to be representative of the upper Florida Current water which is rapidly returned to the upper Mid-Ocean region and $\theta_{South} = 4.5°$C to be the typical potential temperature of NADW returned to 26.5°N below 1000 m depth in the model. Given that we have highlighted above that the greater shallow return flow in the model makes a negligible contribution to the total heat transport across 26.5°N, our revised estimate of the total meridional heat transport, correcting for the model's 1.9 Sv underestimation of vertical overturning, is then given by $Q + Q_s = 0.98$ PW + 0.17 PW = 1.15 PW. Importantly, since our Lagrangian analysis has demonstrated that in order for inflow to the upper Florida Current to form NADW it must participate in both the Subtropical Mode Water (STMW) and NADW diapycnal overturning cells, we would not expect our revised total heat transport estimate to impact the relative heat transport contributions of the STMW (37%) and NADW (63%) overturning cells identified in our study.

References

Aldama-Campino, A., Döös, K., Kjellsson, J., & Jönsson, B. (2020). *TRACMASS: Formal release of version 7.0 (v7.0-beta). Zenodo.* doi: 10.5281/zenodo.4337926

Blanke, B., Arhan, M., Madec, G., & Roche, S. (1999). Warm Water Paths in the Equatorial Atlantic as Diagnosed with a General Circulation Model. *Journal of Physical Oceanography*, *29*(11), 2753 – 2768. (Place: Boston MA, USA Publisher: American Meteorological Society) doi: https://doi.org/10.1175/1520-0485(1999)029⟨2753:WWPITE⟩2.0.CO;2

Döös, K., Jönsson, B., & Kjellsson, J. (2017). Evaluation of oceanic and atmospheric trajectory schemes in the TRACMASS trajectory model v6.0. *Geoscientific Model Development*, *10*(4), 1733–1749. doi: 10.5194/gmd-10-1733-2017

Döös, K., Nycander, J., & Coward, A. C. (2008). Lagrangian decomposition of the Deacon Cell. *Journal of Geophysical Research: Oceans*, *113*(C7). (_eprint: https://agupubs.onlinelibrary.wiley.com/doi/pdf/10.1029/2007JC004351) doi: https://doi.org/10.1029/2007JC004351

Johns, W., Baringer, M., Beal, L., Cunningham, S., Kanzow, T., Bryden, H., … Curry, R. (2011). Continuous, Array-Based Estimates of Atlantic Ocean Heat Transport at 26.5°N. *Journal of Climate*, *24* (10), 2429 – 2449. (Place: Boston MA, USA Publisher: American Meteorological Society) doi: https://doi.org/10.1175/2010JCLI3997.1

Meinen, C. S., Baringer, M. O., & Garcia, R. F. (2010). Florida Current transport variability: An analysis of annual and longer-period signals. *Deep Sea Research Part I: Oceanographic Research Papers*, *57* (7), 835–846. doi: https://doi.org/10.1016/j.dsr.2010.04.001

Moat, B. I., Josey, S. A., Sinha, B., Blaker, A. T., Smeed, D. A., McCarthy, G. D., … Coward, A. C. (2016). Major variations in subtropical North Atlantic heat transport at short (5 day) timescales and their causes. *Journal of Geophysical Research: Oceans*, *121* (5), 3237–3249. (_eprint: https://agupubs.onlinelibrary.wiley.com/doi/pdf/10.1002/2016JC011660) doi: https://doi.org/10.1002/2016JC011660

Tooth, O., Johnson, H., Wilson, C., & Evans, D. (2023). Seasonal overturning variability in the eastern north atlantic subpolar gyre: a lagrangian perspective. *Ocean Science*, *19* (3), 769–791. doi: 10.5194/os-19-769-2023

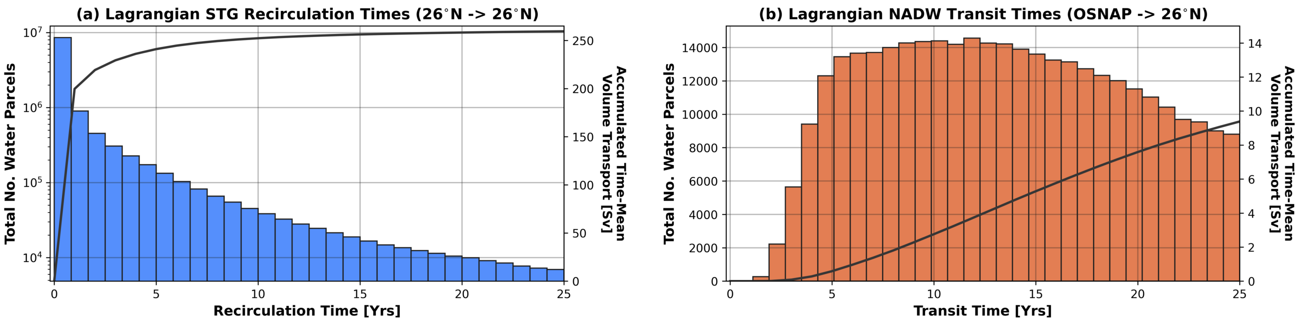

Figure S1. (a) Distribution of recirculation times (years) for all of the water parcels returning to the RAPID 26.5°N section within the 25-year maximum advection period. Note that the total number of recirculating water parcels is shown on a logarithmic scale. The solid black line overlaid depicts how the time-mean volume transport (Sv) initialised along the subtropical gyre pathway is accumulated as a function of water parcel recirculation time. (b) Distribution of transit times (years) taken for water parcels to reach the OSNAP East or West section following initialisation at the RAPID 26.5°N section. The solid black line shows the time-mean volume transport (Sv) accumulated as a function of water parcel transit time and is calculated analogously to in panel (a).

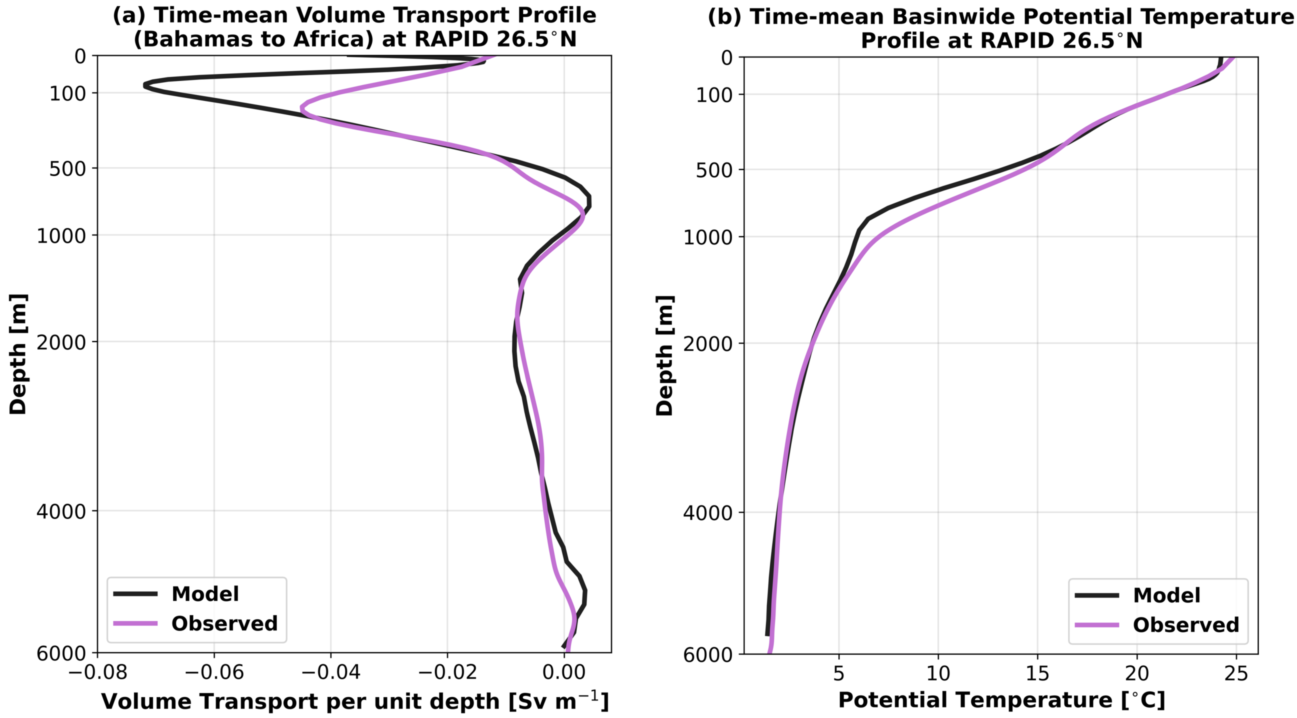

Figure S2. (a) Time-mean (2004-2015) meridional volume transport per unit depth (Sv m^{-1}) in the region between the Bahamas and Africa in the ORCA0083-N06 ocean sea-ice hindcast simulation (model, black) and from RAPID observations (observed, pink). (b) Time-mean (2004-2015) potential temperature profiles (°C) for the entire basin (Straits of Florida to Africa) in the ORCA0083-N06 hindcast (black) and from RAPID observations (pink).

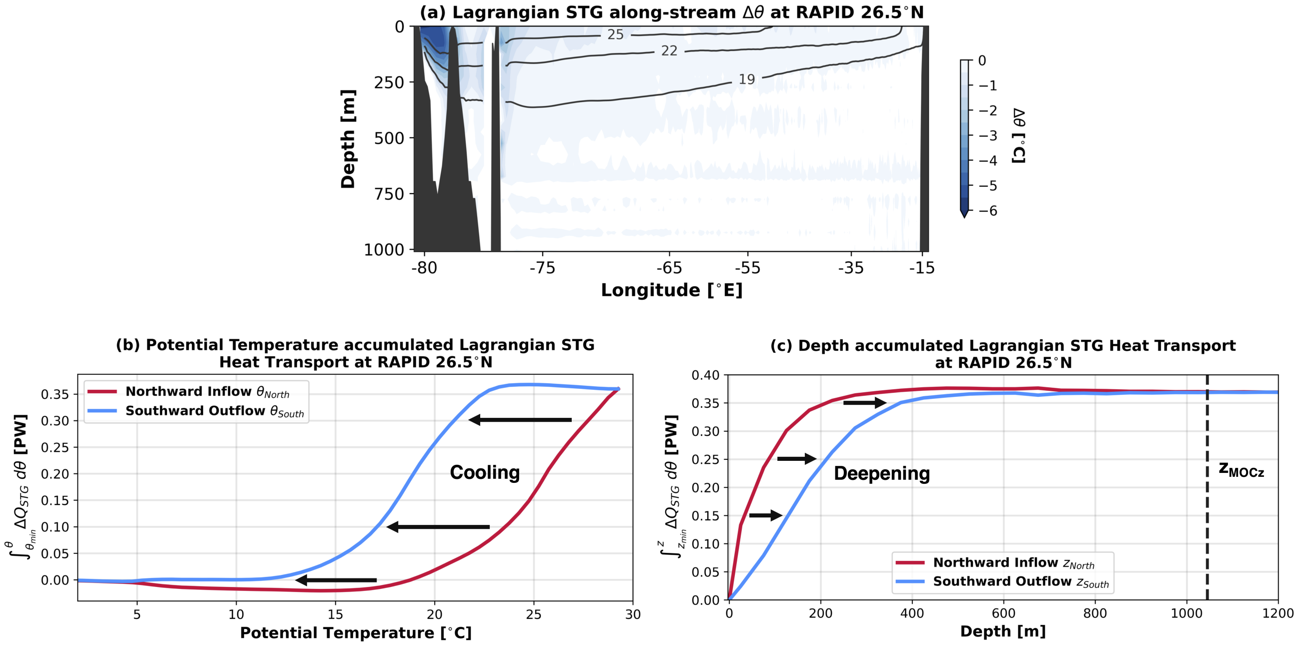

Figure S3. (a) Time-mean net change in potential temperature of water parcels recirculating in the subtropical gyre shown at their northward inflow locations along the RAPID 26.5°N section. Overlaid are isotherms of the time-mean (2004-2015) potential temperature field across the section. (b) Lagrangian heat transport due to the subtropical gyre circulation at 26.5°N accumulated as a function of the potential temperature of recirculating water parcels on their northward (red, θ_{North}) and southward (blue, θ_{South}) crossings of the RAPID section. The value of each curve at a given potential temperature θ informs us how much the collection of recirculating water parcels with an associated northward or southward potential temperature $\leq \theta$ contribute to the time-mean heat transport of the subtropical gyre circulation at 26.5°N. (c) Lagrangian heat transport due to the subtropical gyre circulation at 26.5°N accumulated as a function of the depth of recirculating water parcels on their northward (red, θ_{North}) and southward (blue, θ_{South}) crossings of the RAPID section. The depth of maximum Eulerian overturning, $z_{MOC_z} = 1045$ m, in depth-coordinates, delimiting the upper and lower limbs of the large-scale AMOC, is indicated by black dashed line.

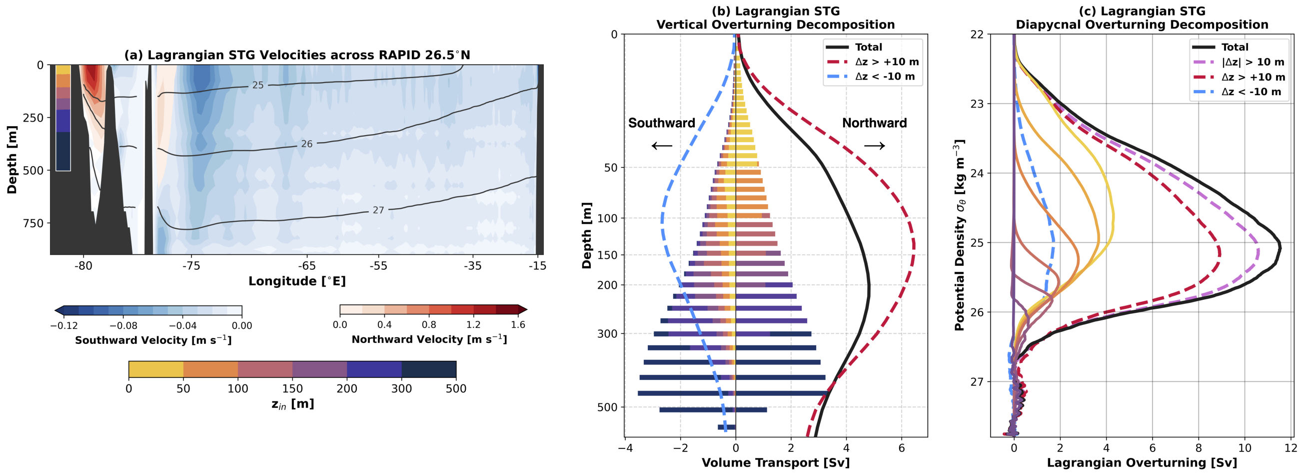

Figure S4. (a) Distribution of subtropical gyre water parcel northward (red contours) and southward (blue contours) crossings of the RAPID 26.5°N section. Contours, shown in m s^{-1}, are computed by summing the total volume transport through each model grid cell and normalising by their area. Water parcel are further classified into six unevenly spaced vertical layers according to their depth on flowing northward across the RAPID section: 0-50 m, 50-100 m, 100-150 m, 150-200 m, 200-300 m, and 300-500m m. (b) Decomposition of the northward and southward volume transports of the subtropical gyre recirculation across 26.5°N according to the vertical layer water parcels flow northward across the RAPID section. The time-mean Lagrangian vertical overturning streamfunction (black) of the subtropical gyre is further partitioned into the contributions made by water parcels which experience a depth change ($|\Delta z|$) $>$ 10 m (downwelling, red) and those which experience a depth change < -10 m (upwelling, blue). (c) Decomposition of the subtropical gyre time-mean Lagrangian diapycnal overturning streamfunction according to the vertical layer water parcels flow northward across 26.5°N. The time-mean Lagrangian diapycnal overturning streamfunction (black) is further partitioned into the contributions of downwelling (red), upwelling (blue) and vertically overturned (pink, total of downwelling and upwelling water parcels since both imprint onto the time-mean vertical overturning at RAPID). The residual between the total time-mean Lagrangian diapycnal overturning streamfunction and the component associated with the vertical overturning circulation of the subtropical gyre is the diapycnal overturning due to horizontal recirculation along constant isobaths.

Table T1.

Time-mean (± std.) volume transports initialised along Lagrangian pathways north of the RAPID 26.5°N section (2004-2015). Lagrangian trajectories which return to 26.5°N within the 25-year maximum advection time are referred to at Subtropical Gyre (STG) water parcels. Water parcels which are sourced from the Overturning in the Subpolar North Atlantic Program (OSNAP) arrays are referred to as North Atlantic Deep Water (NADW). Water parcels sourced from the English Channel (EC) and the Gibraltar Strait (GS) are referred to as GS + EC. The remaining trajectories, which fail to reach any of the boundaries in our Lagrangian experiment domain within the 25-year maximum advection period, are collectively referred to as No Exit water parcels.

Lagrangian Pathway	Volume Transport (Sv)
Total	284.24 ± 25.3
26.5°N -> 26.5°N [STG]	259.52 ± 24.73
OSNAP -> 26.5°N [NADW]	9.40 ± 2.91
GS + EC -> 26.5°N [GS + EC]	0.04 ± 0.03
No Exit	15.29 ± 4.43